Nuclear Physics B299 (1988) 407–430
North-Holland, Amsterdam

GAUGINO-HIGGSINO MIXING AND SLEPTON-SQUARK PRODUCTION IN ep COLLISIONS

H. KOMATSU*

Institut für Physik, Universität Dortmund, FR Germany

R. RÜCKL

Deutsches Elektronen-Synchrotron DESY, Hamburg, FR Germany

Received 25 August 1987

We consider gaugino-higgsino mixing in the minimal supersymmetric extension of the standard model and determine the mass eigenstates and eigenvalues taking the physical masses of the lightest chargino and neutralino as input in the diagonalization procedure. Using the results we calculate cross sections and charge asymmetries for the associated production of sleptons and squarks in ep collisions and investigate the dependence on the chargino and neutralino properties and on the slepton and squark spectrum. The numerical analysis is performed within the minimal supergravity model as well as in a more general framework. Although predictions are made also for higher energies, the main focus is on the HERA energy range. We indicate the values of sparticle masses accessible to SUSY searches at HERA and illustrate the expected reach beyond the present bounds.

1. Introduction

The associated production of a scalar lepton ($\tilde{e}$ or $\tilde{\nu}$) and a scalar quark ($\tilde{q}$) constitutes the most important process in the search for supersymmetry in ep collisions as it provides the clearest signatures and allows to explore the largest mass range of supersymmetric particles. The transitions of the initial electron and quark into sleptons and squarks proceed by t-channel exchange of gauginos and higgsinos, the spin-$\frac{1}{2}$ partners of the electroweak gauge bosons and the Higgs bosons, respectively. In the minimal supersymmetric extension of the standard $SU(3)_c \times SU(2)_L \times U(1)$ theory [1], which contains two Higgs doublets, the charged-current-type processes $eq \to \tilde{\nu}\tilde{q}$ are mediated by wino $\tilde{W}^{\mp}$ and charged higgsino $\tilde{H}_1^-$ and $\tilde{H}_2^+$ exchange, while the neutral-current-type processes $eq \to \tilde{e}\tilde{q}$ involve the neutral $SU(2)_L$ and $U(1)$ gauginos $\tilde{W}^3$ and $\tilde{B}$ and the neutral higgsino fields $\tilde{H}_1^0$ and $\tilde{H}_2^0$.

* Supported by the Deutsche Forschungsgemeinschaft.

0550-3213/88/$03.50 © Elsevier Science Publishers B.V.
(North-Holland Physics Publishing Division)

The couplings of the above $SU(2)_L \times U(1)$ eigenstates are fixed by gauge invariance and supersymmetry and are related to the corresponding gauge and Higgs boson couplings. Since it is justified to take $m_e, m_q \to 0$ in the case of $ep \to \tilde{\ell}\tilde{q}X$, we only have to deal with gaugino couplings later on. Masses can be generated as usual through spontaneous $SU(2)_L \times U(1)$ breaking. However, in order to agree with observations supersymmetry must also be broken. In view of the missing experimental evidence for supersymmetry it is not surprising that the SUSY breaking mechanism is unclear. A possible dynamical framework is provided by supergravity models [1,2]. These models lead to effective low energy lagrangians with global supersymmetry broken by so-called soft breaking terms originating in gravitational interactions. Together with $SU(2)_L \times U(1)$ breaking which can also be induced dynamically in such schemes, these terms generate the mass spectrum of the superpartners. As a characteristic feature, the mass eigenstates are mixtures of $SU(2)_L \times U(1)$ eigenstates with mass eigenvalues and mixing angles depending on a more or less large number of model parameters. This fact renders predictions of SUSY processes somewhat uncertain.

The mixing of the scalar partners $\tilde{f}_L$ and $\tilde{f}_R$ of the left- and right-handed fermions $f_{L,R} = \frac{1}{2}(1 \mp \gamma_5)f$ is expected [1] in supergravity models to be proportional to the fermion masses. Since only light leptons and quarks play an important role in $ep \to \tilde{\ell}\tilde{q}X$, $\tilde{f}_L$-$\tilde{f}_R$ mixing will be neglected throughout this paper. Also flavor mixing has no essential influence on our analysis as will become clear later. On the other hand, the mixing of gauginos and higgsinos is typically substantial. The charged mass eigenstates $\tilde{\chi}_{Ci}$ $(i = 1, 2)$ being mixtures of $\tilde{W}^-(\tilde{W}^+)$ and $\tilde{H}_1^-(\tilde{H}_2^+)$ are called charginos, while the neutral mass eigenstates $\tilde{\chi}_{Ni}$ $(i = 1, 2, 3, 4)$ being mixtures of $\tilde{B}$, $\tilde{W}^3$, $\tilde{H}_1^0$ and $\tilde{H}_2^0$ are called neutralinos. It is the main purpose of this paper to study chargino and neutralino spectra in the mass range accessible at HERA, to investigate the model-dependence of the cross sections for $ep \to \tilde{\ell}\tilde{q}X$, and to estimate the range of slepton and squark masses and other model parameters which can be explored at HERA energies.

Already some time ago, Jones and Llewellyn Smith [3] calculated cross sections for $ep \to \tilde{\ell}\tilde{q}X$ considering wino ($\tilde{W}^{\pm}$), zino ($\tilde{Z}$) and photino ($\tilde{\gamma}$) exchange in the absence of gaugino-higgsino mixing. The above gauginos are the superpartners of the W and Z bosons and the photon, respectively, as it is evident from their definition

$$\tilde{W}^{\pm} = \sqrt{\tfrac{1}{2}}\left(\tilde{W}^1 \mp i\tilde{W}^2\right),$$

$$\tilde{Z} = \cos\theta_W \tilde{W}^3 - \sin\theta_W \tilde{B},$$

$$\tilde{\gamma} = \sin\theta_W \tilde{W}^3 + \cos\theta_W \tilde{B} \tag{1}$$

in terms of the $SU(2)_L$ gaugino fields $\tilde{W}^i$ $(i = 1, 2, 3)$ and the U(1) gaugino $\tilde{B}$ with θ_W being the Weinberg angle. Although one can approximate this case by diagonalizing the gaugino/higgsino mass matrices under rather special assumptions, it does not occur as a typical solution and not for the mass eigenvalues $m_{\tilde{W}} \simeq m_W$, $m_{\tilde{Z}} \simeq m_Z$ and $m_{\tilde{\gamma}} \simeq 0$ assumed in ref. [3], at least not in the minimal model as will be seen. Gaugino-higgsino mixing was later included by Harrison [4] who emphasized the considerable sensitivity of the production cross sections for ep $\to \tilde{\ell}\tilde{q}X$ to mixing and demonstrated this point for a few special cases. Our aim is a more comprehensive study which improves, extends and corrects the earlier analyses in several respects:

(i) Instead of diagonalizing the gaugino/higgsino mass matrices for given values of the various mass parameters which appear in the effective lagrangian, we use the desired mass values of the lightest neutralino and chargino eigenstates as input in the diagonalization problem and determine the gaugino/higgsino composition of the eigenstates and the heavier masses from these directly observable parameters under assumptions on the remaining parameters which are suggested by renormalization group considerations within supergravity models and which will be specified later. The phenomenological advantages of such a procedure are quite obvious.

(ii) We investigate the total ep $\to \tilde{\ell}\tilde{q}X$ cross sections for many interesting chargino and neutralino solutions and clarify the dependence of the cross sections on slepton and squark masses and on the chargino and neutralino spectra. This analysis is performed in a more general framework with basically free scalar masses as well as for sparticle spectra obeying the renormalization group mass relations [5] of the minimal supergravity model.

(iii) We indicate the region of the parameter space of the supergravity model which can be probed at HERA in comparison to the already existing experimental bounds.

(iv) Charge asymmetries derived from the cross sections for $e^{\mp}p \to \tilde{\ell}\tilde{q}X$ are also investigated. These asymmetries provide particularly sensitive tests of the chargino and neutralino properties.

(v) We have recalculated the cross sections tabulated in ref. [4] using essentially the same values of parameters. In most cases we reproduce the results within a few percent and in some cases within 30%. However, in a few cases we disagree by a factor 2 and more.

The paper is organized as follows. Sect. 2 deals with gaugino/higgsino mixing and the determination of chargino and neutralino eigenstates and masses. In sect. 3 we summarize analytical formulas which are useful for cross section calculations. Our numerical results are presented and discussed in sect. 4. Sect. 5, finally, contains some concluding remarks.

2. Gaugino-higgsino mixing

In the minimal supersymmetric $SU(2)_L \times U(1)$ model [1,2], two $SU(2)_L$ Higgs doublets $H_1 = (H_1^0, H_1^-)$ and $H_2 = (H_2^+, H_2^0)$ exist with opposite U(1) hypercharge.

The neutral Higgs fields $H^0_{1,2}$ acquire non-vanishing vacuum expectation values $v_{1,2}$ which break $SU(2)_L \times U(1)$ to $U(1)_{em}$. The higgsino superpartners $\tilde{H}_1 = (\tilde{H}^0_1, \tilde{H}^-_1)$ and $\tilde{H}_2 = (\tilde{H}^+_2, \tilde{H}^0_2)$ of the Higgs-doublets mix with the $SU(2)_L \times U(1)$ gauginos $\tilde{W}^i$ $(i = 1,2,3)$ and $\tilde{B}$ through the spontaneous breakdown of $SU(2)_L \times U(1)$. Going from the two-component spinor notation tacitly assumed above to a four-component notation, one may choose the Dirac spinors

$$\tilde{\psi}_{C1} = \left(\frac{\tilde{W}^-}{\overline{\tilde{W}^+}} \right), \qquad \tilde{\psi}_{C2} = \left(\frac{\tilde{H}^-_1}{\overline{\tilde{H}^+_2}} \right) \tag{2}$$

and the Majorana spinors

$$\tilde{\psi}_{N1} = \left(\frac{\tilde{\gamma}}{\overline{\tilde{\gamma}}} \right), \qquad \tilde{\psi}_{N2} = \left(\frac{\tilde{Z}}{\overline{\tilde{Z}}} \right), \qquad \tilde{\psi}_{N3} = \left(\frac{\tilde{H}}{\overline{\tilde{H}}} \right), \qquad \tilde{\psi}_{N4} = \left(\frac{\tilde{H}'}{\overline{\tilde{H}'}} \right) \tag{3}$$

as the basis of the gaugino-higgsino system, where $\tilde{W}^\pm$, $\tilde{Z}$ and $\tilde{\gamma}$ are defined in eq. (1) and

$$\begin{aligned} \tilde{H} &= \cos\theta_v \tilde{H}^0_1 - \sin\theta_v \tilde{H}^0_2 , \\ \tilde{H}' &= \sin\theta_v \tilde{H}^0_1 + \cos\theta_v \tilde{H}^0_2 \end{aligned} \tag{4}$$

with

$$\tan\theta_v = v_2/v_1 . \tag{5}$$

The most general gaugino-higgsino mass lagrangian [1] of the effective theory can then be written as follows:

$$\mathcal{L}_m = -\bar{\tilde{\psi}}_{Ci}\left(M^C_{ij} P_L + M^{C*}_{ji} P_R \right) \tilde{\psi}_{Cj} - \tfrac{1}{2} \bar{\tilde{\psi}}_{Ni}\left(M^N_{ij} P_L + M^{N*}_{ij} P_R \right) \tilde{\psi}_{Nj} . \tag{6}$$

Here, $P_{L,R} = \frac{1}{2}(1 \mp \gamma_5)$ are the chiral projection operators and the non-diagonal mass matrices M^C_{ij} and M^N_{ij} read

$$M^C = \begin{pmatrix} M_2 & i\sqrt{2}\, m_W \cos\theta_v \\ i\sqrt{2}\, m_W \sin\theta_v & -\mu \end{pmatrix} \tag{7}$$

and

$$M^N = \begin{pmatrix} M_{11} & M_{12} & 0 & 0 \\ M_{12} & M_{22} & i m_Z & 0 \\ 0 & i m_Z & -\mu \sin 2\theta_v & \mu \cos 2\theta_v \\ 0 & 0 & \mu \cos 2\theta_v & \mu \sin 2\theta_v \end{pmatrix} , \tag{8}$$

with

$$M_{11} = \cos^2\theta_W M_1 + \sin^2\theta_W M_2\,,$$

$$M_{22} = \sin^2\theta_W M_1 + \cos^2\theta_W M_2\,,$$

$$M_{12} = (M_2 - M_1)\sin\theta_W \cos\theta_W\,. \tag{9}$$

The generally complex mass parameters M_1, M_2 and μ in the above are soft SUSY breaking parameters associated with the U(1) and $\mathrm{SU(2)_L}$ gauginos and with the higgsinos, respectively, while m_W and m_Z denote the physical W and Z boson masses.

The mass matrices (7) and (8) can be diagonalized by unitary matrices U_L, U_R and U_N,

$$\left(U_R^{\dagger} M^C U_L\right)_{ij} = m_{Ci}\,\delta_{ij}\,, \tag{10}$$

$$\left(U_N^{T} M^N U_N\right)_{ij} = m_{Ni}\,\delta_{ij}\,, \tag{11}$$

with the (positive) eigenvalues m_{Ci} and m_{Ni} being the masses of the chargino ($\tilde{\chi}_{Ci}$, $i = 1,2$) and neutralino ($\tilde{\chi}_{Ni}$, $i = 1,2,3,4$) mass eigenstates. These states are obtained from the basis defined in eqs. (2) and (3) by the transformations

$$P_L\tilde{\chi}_C = U_L^{\dagger} P_L \tilde{\psi}_C\,, \qquad P_R\tilde{\chi}_C = U_R^{\dagger} P_R \tilde{\psi}_C\,, \tag{12}$$

$$P_L\tilde{\chi}_N = U_N^{\dagger} P_L \tilde{\psi}_N\,, \qquad P_R\tilde{\chi}_N = U_N^{T} P_R \tilde{\psi}_N\,. \tag{13}$$

The mass lagrangian (6) then takes the simple form

$$\mathscr{L}_m = -m_{Ci}\bar{\tilde{\chi}}_{Ci}\tilde{\chi}_{Ci} - \tfrac{1}{2} m_{Ni}\bar{\tilde{\chi}}_{Ni}\tilde{\chi}_{Ni}\,. \tag{14}$$

In order to determine the physical chargino and neutralino states and their masses one must know M_1, M_2, μ and θ_v, in other words, the model must be further specified. As reasonable assumptions, we shall adopt the following three constraints:

(a) $$\cos 2\theta_v = 0\,,$$

(b) $$3M_1\cos^2\theta_W = 5M_2\sin^2\theta_W\,,$$

(c) $$M_1,\ M_2 \text{ and } \mu \text{ real}\,. \tag{15}$$

Assumption (a) is suggested by a renormalization group analysis of a class of supergravity models [2,5] for a top quark mass $m_t \simeq 50$ GeV. Small deviations of $\cos 2\theta_v$ from zero do not alter our result significantly except in a small region of the parameter space where one has a mass degeneracy. Assumption (b) applies if M_1 and M_2 are evolved according to the renormalization group [5] from equal values $M_1 = M_2 = m_{1/2}$ at a grand unification scale M_X down to energies of O(1 TeV). In that case,

$$\frac{1}{g_X^2} m_{1/2} = \frac{1}{g^2} M_2 = \frac{3}{5g'^2} M_1 , \tag{16}$$

where g_X is the unified gauge coupling at M_X and g and g' are the usual effective $SU(2)_L$ and U(1) gauge couplings, respectively, with $g'/g = \tan\theta_W$. Finally, assumption (c) is employed merely for reasons of simplicity. Adding the specifications (15) to the model, one has to deal with only two unknown real parameters, M_2 and μ.

Instead of choosing certain values for M_2 and μ and deriving the corresponding chargino and neutralino spectrum, we want to proceed in the opposite way and use two physical chargino and neutralino masses as input in the diagonalization problem. Substituting first assumption (15a) in the neutral mass matrix M^N, eq. (8), one immediately sees that the higgsino $\tilde{\psi}_{N4}$ defined in eqs. (3) and (4) does not mix with the other neutral fields $\tilde{\psi}_{Ni}$; $i = 1,2,3$. Hence, according to eqs. (11) and (13), the fourth neutralino eigenstate $\tilde{\chi}_{N4}$ remains a pure higgsino, $\tilde{\chi}_{N4} = \tilde{\psi}_{N4}$, with mass $m_{N4} = |\mu|$, while the other eigenstates $\tilde{\chi}_{Ni}$; $i = 1,2,3$ and their masses m_{Ni} are found by diagonalizing the appropriate 3×3 submatrix of eq. (8). Ordering $\tilde{\chi}_{Ni}$; $i = 1,2,3$ and $\tilde{\chi}_{Ci}$, $i = 1,2$ such that $m_{N1} \leqslant m_{N2} \leqslant m_{N3}$ and $m_{C1} \leqslant m_{C2}$, we choose suitable values for m_{N1} and m_{C1} and solve the eigenvalue equations.

In table 1 we list solutions for a range of values of m_{N1} and m_{C1} which is of particular interest from the point of view of future searches for electroweak SUSY signals, that is the mass range up to O(1 TeV). Also quoted in table 1 are the values of M_2 (with the convention $M_2 \geqslant 0$) and μ associated with a given solution. The following features are noteworthy:

(i) For a fixed value of m_{N1} solutions exist for m_{C1} approximately in the range $m_{N1} \lesssim m_{C1} \lesssim \sqrt{4m_{N1}^2 + m_W^2}$.

(ii) For $0 = m_{N1} < m_{C1}$ there are two solutions which differ in M_2 and μ as well as in the other neutralino and chargino masses and in the composition of the mass eigenstates. On the other hand, for $m_{N1} = m_{C1}$ only one solution yields finite mass values for all states, while for $m_{N1} = 0$, $m_{C1} \lesssim m_W$ one has unique solutions.

(iii) The lightest state ($\tilde{\chi}_{N1}$ by definition) of the neutralinos $\tilde{\chi}_{Ni}$; $i = 1,2,3$ tends to be dominantly a photino or it normally contains at least a large photino component.

(iv) The approximate photino $\tilde{\chi}_{N1}$ is in most cases also lighter than the pure higgsino $\tilde{\chi}_{N4}$, i.e. $m_{N1} < m_{N4}$, except in the degenerate case $m_{N1} = m_{C1}$ where $m_{N4} < m_{N1}$.

(v) The mixing of zino and higgsino components in $\tilde{\chi}_{N2}$ and $\tilde{\chi}_{N3}$ is similar to the mixing of wino and higgsino components in $\tilde{\chi}_{C1}$ and $\tilde{\chi}_{C2}$, respectively. This similarity is also reflected in the mass pattern $m_{N2} \simeq m_{C1}$ and $m_{N3} \simeq m_{C2}$.

TABLE 1

Masses and eigenstates of neutralinos and charginos and the corresponding values of the SUSY breaking parameters M_2 and μ (masses in GeV).

Neutralinos			Charginos		SUSY breaking	
m_{N1} ($U_{N11}, U_{N21}, U_{N31}$)	m_{N2} ($U_{N12}, U_{N22}, U_{N32}$)	m_{N3} ($U_{N13}, U_{N23}, U_{N33}$)	m_{C1} (U_{L11}, U_{L21})	m_{C2}	M_2	μ
0(1.000, 0.0, 0.0)	38(0.000, −0.927i, 0.375)	230(0.000, 0.375, −0.927i)	30(0.939i, −0.345)	222	0.0	192.0
0(1.000, 0.0, 0.0)	60(0.000, 0.839, −0.544i)	143(0.000, −0.544i, 0.839)	50(0.853, −0.522i)	133	0.0	−83.2
0(1.000, 0.0, 0.0)	91(0.000, 0.713, −0.701i)	95(0.000, −0.701i, 0.713)	80(0.714, −0.700i)	83	0.0	−3.2
20(0.103, −0.277, −0.955i)	221(0.895, −0.393, 0.210i)	441(0.434, 0.877, −0.207i)	30(0.203, 0.979i)	441	423.7	46.9
20(0.996, 0.047, 0.077i)	44(0.084i, −0.790i, 0.607)	149(0.032, 0.[illegible]11, −0.791i)	30(0.796i, −0.605)	139	32.1	77.3
20(0.972, −0.231, 0.050i)	52(0.237, 0.952, −0.192i)	429(0.003i, −0.198i, 0.980)	50(0.985, −0.175i)	424	35.5	−410.0
20(0.997, 0.009, 0.074i)	64(0.058i, −0.711i, 0.701)	123(0.047, 0.703, −0.709i)	50(0.703i, −0.711)	113	32.5	30.7
20(0.996, −0.061, 0.069i)	88(0.089, 0.847, −0.524i)	120(0.026i, −0.528i, 0.849)	80(0.868, −0.497i)	109	33.3	−62.7
20(0.997, −0.032, 0.072i)	92(0.038i, −0.608i, 0.793)	101(0.069, 0.793, −0.605i)	80(0.586i, −0.811)	92	33.0	−21.0
50(0.982, −0.089, 0.164i)	64(0.087i, −0.563i, 0.822)	140(0.166, 0.822, −0.545i)	50(0.520i, −0.854)	134	84.1	−0.4
50(0.374, −0.635, −0.676i)	123(0.898, 0.066, 0.436i)	258(0.232, 0.770, −0.595i)	80(0.575, 0.818i)	253	196.1	137.4
50(0.978, −0.145, 0.150i)	92(0.061i, −0.488i, 0.870)	131(0.200, 0.860, −0.469i)	80(0.441i, −0.897)	126	85.9	−39.9
50(0.872, −0.490, −0.008i)	100(0.490, 0.872, 0.014i)	6103(0.000, 0.015, −1.000i)	100(1.000, 0.014i)	6103	101.1	6102.0
50(0.974, −0.175, 0.142i)	111(0.050i, −0.447i, 0.893)	127(0.219, 0.877, −0.427i)	100(0.400i, −0.916)	123	86.9	−64.4
100(0.931, −0.323, 0.170i)	109(0.058i, −0.329i, 0.942)	210(0.361, 0.887, −0.288i)	100(0.275i, −0.961)	209	185.2	−76.6
100(0.582, −0.624, −0.521i)	175(0.775, 0.231, 0.589i)	324(0.247, 0.746, −0.618i)	150(0.601, 0.799i)	320	258.5	211.4
100(0.924, −0.354, 0.143i)	157(0.041i, −0.281i, 0.959)	209(0.379, 0.892, −0.245i)	150(0.235i, −0.972)	208	187.8	−130.3
100(0.872, −0.489, −0.014i)	200(0.490, 0.872, 0.026i)	3317(0.000, 0.030, −1.000i)	200(1.000, 0.026i)	3316	202.1	3314.1
100(0.919, −0.375, 0.123i)	206(0.030i, −0.244i, 0.969)	208(0.393, 0.894, −0.213i)	200(0.205i, −0.979)	207	189.7	−182.9

TABLE 1 (Continued)

Neutralinos			Charginos		SUSY breaking	
m_{N1} $(U_{N11}, U_{N21}, U_{N31})$	m_{N2} $(U_{N12}, U_{N22}, U_{N32})$	m_{N3} $(U_{N13}, U_{N23}, U_{N33})$	m_{C1} (U_{L11}, U_{L21})	m_{C2}	M_2	μ
200(0.893, −0.437, 0.105i)	205(0.032i, −0.171i, 0.985)	404(0.449 , 0.883 , −0.139i)	200(0.136i, −0.991)	404	392.3	−188.8
200(0.760, −0.552, −0.343i)	314(0.561 , 0.292 , 0.775i)	486(0.327 , 0.782 , −0.531i)	300(0.518 , 0.855i)	484	434.7	349.4
200(0.891, −0.446, 0.085i)	304(0.022i, −0.144i, 0.989)	404(0.454 , 0.883 , −0.118i)	300(0.117i, −0.993)	404	394.1	−290.4
200(0.873, −0.488, −0.023i)	400(0.488 , 0.871 , 0.047i)	2139(0.002 , 0.052 , −0.999i)	400(0.999 , 0.047i)	2138	403.8	2133.9
200(0.889, −0.452, 0.071i)	403(0.016i, −0.124i, 0.992)	404(0.457 , 0.883 , −0.103i)	400(0.102i, −0.995)	404	395.4	−391.6
400(0.882, −0.469, 0.055i)	402(0.016i, −0.086i, 0.996)	804(0.472 , 0.879 , −0.068i)	400(0.068i, −0.998)	804	798.6	−394.4
400(0.840, −0.504, −0.204i)	609(0.347 , 0.209 , 0.914i)	853(0.418 , 0.838 , −0.350i)	600(0.345 , 0.939i)	852	822.1	630.0
400(0.881, −0.471, 0.044i)	602(0.011i, −0.072i, 0.997)	804(0.473 , 0.879 , −0.058i)	600(0.058i, −0.998)	804	799.5	−595.2
400(0.874, −0.485, −0.031i)	800(0.486 , 0.871 , 0.076i)	1877(0.010 , 0.081 , −0.997i)	800(0.997 , 0.076i)	1875	806.2	1869.2
400(0.880, −0.473, 0.037i)	802(0.008i, −0.062i, 0.998)	804(0.474 , 0.879 , −0.051i)	800(0.051i, −0.999)	804	800.2	−795.8
800(0.879, −0.477, 0.028i)	801(0.008i, −0.043i, 0.999)	1607(0.478 , 0.878 , −0.034i)	800(0.034i, −0.999)	1607	1604.5	−797.2
800(0.867, −0.486, −0.109i)	1205(0.188 , 0.117 , 0.975i)	1633(0.461 , 0.866 , −0.193i)	1200(0.192 , 0.981i)	1633	1616.8	1216.0
800(0.878, −0.477, 0.022i)	1201(0.006i, −0.036i, 0.999)	1607(0.478 , 0.878 , −0.029i)	1200(0.029i, −1.000)	1607	1605.0	−1197.6
800(0.876, −0.482, −0.030i)	1600(0.482 , 0.868 , 0.117i)	2301(0.030 , 0.117 , −0.993i)	1600(0.993 , 0.117i)	2300	1609.7	2289.9
800(0.878, −0.478, 0.019i)	1601(0.004i, −0.031i, 1.000)	1607(0.478 , 0.878 , −0.025i)	1600(0.025i, −1.000)	1607	1605.3	−1597.9

The mass values m_{N1} and m_{C1} and the constraints eq. (15) are used as input in the diagonalization of the mass matrices M^C and M^N given in eqs. (7) and (8). The neutralino eigenstates $\tilde{\chi}_{Ni}$, $i = 1,\ldots,4$ are characterized by the vectors $(U_{N1i}, U_{N2i}, U_{N3i}, U_{N4i})$ where the elements U_{Nji}, $j = 1,\ldots,4$ of the diagonalization matrix in eq. (11) describe the $\tilde{\gamma}$, $\tilde{Z}$, $\tilde{H}$ and $\tilde{H}'$ admixture, respectively. The vanishing components U_{N4i}, $i = 1,2,3$ and the unmixed state $\tilde{\chi}_{N4}$ which has the mass $m_{N4} = |\mu|$ are not shown. Similarly, the chargino eigenstates $\tilde{\chi}_{Ci}$; $i = 1,2$ are given by the vectors (U_{L1i}, U_{L2i}) where the elements $U_{Lji} = U^*_{Rji}$, $j = 1,2$ of the diagonalization matrices in eq. (10) refer to the $\tilde{W}^{\pm}$ and $\tilde{H}^{\pm}$ components, respectively. The state $\tilde{\chi}_{C2}$ not shown can be obtained from $\tilde{\chi}_{C1}$ as follows: $U_{L12} = -i\varepsilon U_{L21}|U_{L11}|/U_{L11}$ and $U_{L22} = -i\varepsilon|U_{L11}|$ with $\varepsilon = 1$ for $M_2 + \mu > 0$ and $\varepsilon = i$ for $M_2 + \mu < 0$.

One can easily understand these properties by considering the limit $\sin^2\theta_W \to 0$. In this limit, the photino $\tilde{\psi}_{N1}$ does not get mixed with the other neutral fields, i.e. $\tilde{\chi}_{N1} = \tilde{\psi}_{N1}$, and the mass matrix of $\tilde{\psi}_{N2}$ and $\tilde{\psi}_{N3}$ becomes identical to the chargino mass matrix as can be seen from eqs. (7) and (8). Hence, the neutralino masses assume the values

$$m_{N1} = M_1, \qquad m_{N2} = m_{C1}, \qquad m_{N3} = m_{C2}, \qquad m_{N4} = |\mu|, \tag{17}$$

while the chargino masses are given by

$$m_{C1,C2} = \tfrac{1}{2}\left| M_2 + \mu \pm \sqrt{(M_2 - \mu)^2 + 4m_W^2} \right| \tag{18}$$

with the convention $m_{C1} \leqslant m_{C2}$. Furthermore, we note the approximate numerical relation

$$M_1 = \tfrac{5}{3}\tan^2\theta_W M_2 \simeq \tfrac{1}{2}M_2. \tag{19}$$

At small values of m_{N1}, the mass spectrum (17) is considerably distorted due to effects of the non-vanishing Weinberg angle $\sin^2\theta_W = 0.23$. However, already for $m_{N1} \gtrsim 100$ GeV eq. (17) becomes a very good approximation. Similarly, one expects the neutralino and chargino eigenstates to approach the limits

$$\begin{aligned}
&\tilde{\chi}_{N1} \to \tilde{B} = \cos\theta_W \tilde{\gamma} - \sin\theta_W \tilde{Z}, \\
&\tilde{\chi}_{N2} \to \tilde{H} \quad \text{or} \quad \tilde{W}^3 = \sin\theta_W \tilde{\gamma} + \cos\theta_W \tilde{Z}, \\
&\tilde{\chi}_{N3} \to \tilde{W}^3 \quad \text{or} \quad \tilde{H} = \sqrt{\tfrac{1}{2}}\left(\tilde{H}_1^0 - \tilde{H}_2^0\right), \\
&\left(\tilde{\chi}_{N4} = \tilde{H}' = \sqrt{\tfrac{1}{2}}\left(\tilde{H}_1^0 + \tilde{H}_2^0\right)\right),
\end{aligned} \tag{20}$$

and

$$\begin{aligned}
&\tilde{\chi}_{C1} \to \tilde{H}_{1,2}^{\mp} \quad \text{or} \quad \tilde{W}^{\mp}, \\
&\tilde{\chi}_{C2} \to \tilde{W}^{\mp} \quad \text{or} \quad \tilde{H}_{1,2}^{\mp},
\end{aligned} \tag{21}$$

respectively. This is obviously the case for the numerical solutions given in table 1.

3. Calculation of cross sections

Our next task is to derive cross-section formulas for slepton-squark production in ep collisions which take into account gaugino-higgsino mixing. To recapitulate, the couplings of the $SU(2)_L \times U(1)$ gauginos to fermion-sfermion pairs are related to the standard gauge boson-fermion couplings, while the higgsino-fermion-sfermion interactions are of Yukawa type similar to the familiar couplings of Higgs bosons to fermions. Since the latter are proportional to lepton and quark masses, higgsino couplings can safely be neglected in $eq \to \tilde{\ell}\tilde{q}$, the elementary processes we are dealing with. Then, writing the gaugino-fermion-sfermion lagrangian [1] of the effective theory in terms of the chargino and neutralino mass eigenstates defined in eqs. (12) and (13), one gets

$$\mathscr{L}_{\mathrm{int}} = -i\left(\eta^{\mathrm{C}}_{\mathrm{u_L}}\right)_i \tilde{d}^*_{\mathrm{L}}\bar{\tilde{\chi}}^{\mathrm{c}}_{\mathrm{C}i} u_{\mathrm{L}} - i\left(\eta^{\mathrm{C}}_{\mathrm{d_L}}\right)_i \tilde{u}^*_{\mathrm{L}}\bar{\tilde{\chi}}_{\mathrm{C}i} d_{\mathrm{L}}$$

$$-i\left(\eta^{\mathrm{N}}_{\mathrm{f_L}}\right)_i \tilde{f}^*_{\mathrm{L}}\bar{\tilde{\chi}}_{\mathrm{N}i} f_{\mathrm{L}} - i\left(\eta^{\mathrm{N}}_{\mathrm{f_R}}\right)_i \tilde{f}^*_{\mathrm{R}}\bar{\tilde{\chi}}_{\mathrm{N}i} f_{\mathrm{R}} + \mathrm{h.c.}, \tag{22}$$

with

$$\left(\eta^{\mathrm{C}}_{\mathrm{u_L}}\right)_i = \frac{e}{\sin\theta_{\mathrm{W}}}(U_{\mathrm{L}})_{1i}, \tag{23a}$$

$$\left(\eta^{\mathrm{C}}_{\mathrm{d_L}}\right)_i = \frac{e}{\sin\theta_{\mathrm{W}}}(U^*_{\mathrm{R}})_{1i}, \tag{23b}$$

$$\left(\eta^{\mathrm{N}}_{\mathrm{f_L}}\right)_i = \sqrt{2}\, e\left[Q_{\mathrm{f}}(U_{\mathrm{N}})_{1i} + \frac{T_{3\mathrm{f}} - Q_{\mathrm{f}}\sin^2\theta_{\mathrm{W}}}{\sin\theta_{\mathrm{W}}\cos\theta_{\mathrm{W}}}(U_{\mathrm{N}})_{2i}\right], \tag{24a}$$

$$\left(\eta^{\mathrm{N}}_{\mathrm{f_R}}\right)_i = \sqrt{2}\, eQ_{\mathrm{f}}\left[(U^*_{\mathrm{N}})_{1i} - \tan\theta_{\mathrm{W}}(U^*_{\mathrm{N}})_{2i}\right]. \tag{24b}$$

In the above, u and d denote the up-type fermions (ν_{e}, u; ν_μ, c; etc.) and the down-type fermions (e, d; μ, s; etc.), respectively, while f refers to both u and d. The scalar partners are correspondingly denoted by $\tilde{\mathrm{u}}$, $\tilde{\mathrm{d}}$ and $\tilde{\mathrm{f}}$. Summation over lepton and quark flavors is implied in eq. (22) and is obvious. Furthermore, the subscripts L and R mark the left- and right-handed fermion components $\mathrm{f}_{\mathrm{L,R}} = \frac{1}{2}(1 \mp \gamma_5)\mathrm{f}$ and their superpartners $\tilde{\mathrm{f}}_{\mathrm{L,R}}$, whereas the labels C and N distinguish chargino and neutralino quantities. The field $\tilde{\chi}^{\mathrm{c}}$ is the charge conjugate of $\tilde{\chi}$. Finally, the effective couplings given in eqs. (23) and (24) involve the electromagnetic coupling constant e, the electromagnetic charges Q_{f} (with the convention $Q_{\mathrm{e}} = -1$), the third components of the weak isospin $T_{3\mathrm{f}}$ and elements of the diagonalization matrices U_{L}, U_{R} and U_{N} defined in eqs. (10)–(13).

More specifically, $(U_{\mathrm{L}})_{1i}$ and $(U_{\mathrm{R}})_{1i}$ in eq. (23) characterize the wino admixture in the chargino eigenstates $\tilde{\chi}_{\mathrm{C}i}$; $i = 1, 2$, while $(U_{\mathrm{N}})_{1i}$ and $(U_{\mathrm{N}})_{2i}$ in eq. (24) describe the photino and zino components in the neutralino eigenstates $\tilde{\chi}_{\mathrm{N}i}$; $i = 1, 2, 3, 4$, respectively. Since higgsino Yukawa couplings are neglected, the elements $(U_{\mathrm{L}})_{2i}$, $(U_{\mathrm{R}})_{2i}$ and $(U_{\mathrm{N}})_{3i}$, $(U_{\mathrm{N}})_{4i}$ associated with the higgsino admixtures do not enter eqs. (23) and (24). Further simplifications arise from assumption (15a) which implies $U_{\mathrm{R}} = U^*_{\mathrm{L}}$ and $(U_{\mathrm{N}})_{i4} = 0$ for $i = 1, 2, 3$ reflecting the fact that $\tilde{\chi}_{\mathrm{N}4}$ is a pure higgsino. For reasons pointed out in the introduction we disregard in eq. (22) the possibility of mixing among the scalar partners $\tilde{\mathrm{f}}_{\mathrm{L}}$ and $\tilde{\mathrm{f}}_{\mathrm{R}}$ of the left- and right-handed

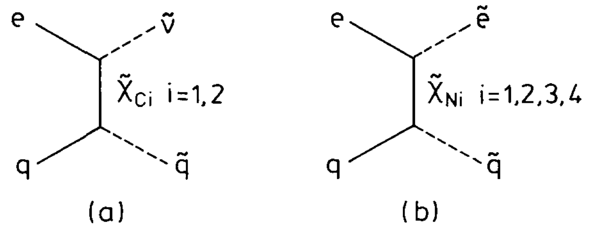

Fig. 1. Schematic diagrams contributing to the inclusive processes (a) ep $\to \tilde{\nu}\tilde{q}X$ and (b) ep $\to \tilde{e}\tilde{q}X$.

helicity components of a fermion field f. Also flavor mixing is suppressed in eq. (22) since it is irrelevant for suitably defined total cross sections because of unitarity if the scalar quarks are mass degenerate. Such a degeneracy is approximately expected in supergravity models [2, 5] and shall be assumed throughout this paper. Scalar top may be an exceptional case which, however, would not influence our numerical analysis of eq $\to \tilde{\ell}\tilde{q}X$ significantly.

With the effective lagrangian (22) it is rather straightforward to compute the differential cross sections for eq $\to \tilde{\ell}\tilde{q}$ according to the diagrams sketched in fig. 1. For an incident electron and quark with the same helicity a = L or R, one obtains [3]

$$\frac{d\sigma}{d\hat{t}}\left(e_a^- q_a \to \tilde{\ell}_a \tilde{q}_a\right) = \frac{1}{16\pi\hat{s}}\left|\sum_i \frac{(\eta_{e_a})_i (\eta_{q_a})_i}{\hat{t}-m_i^2} m_i\right|^2$$

$$= \frac{d\sigma^{aa}(e^- q \to \tilde{\ell}\tilde{q})}{d\hat{t}}, \tag{25}$$

whereas for an incident electron and quark with opposite helicities a = L, b = R or vice versa, one finds [3]

$$\frac{d\sigma}{d\hat{t}}\left(e_a^- q_b \to \tilde{\ell}_a \tilde{q}_b\right) = \frac{1}{16\pi\hat{s}^2}\left|\sum_i \frac{(\eta_{e_a})_i (\eta_{q_b})_i}{\hat{t}-m_i^2}\right|^2$$

$$\times\left[-\hat{t}\hat{s} - \left(m_{\tilde{\ell}}^2 - \hat{t}\right)\left(m_{\tilde{q}}^2 - \hat{t}\right)\right]$$

$$= \frac{d\sigma^{ab}(e^- q \to \tilde{\ell}\tilde{q})}{d\hat{t}}. \tag{26}$$

The scattering variables are defined as usual by

$$\hat{s} = (p_e + p_q)^2, \qquad \hat{t} = (p_e - p_{\tilde{\ell}})^2, \qquad \hat{u} = (p_e - p_{\tilde{q}})^2, \tag{27}$$

with $\hat{s}+\hat{t}+\hat{u}=m_{\tilde{\ell}}^2+m_{\tilde{q}}^2$, $m_{\tilde{\ell}}$ and $m_{\tilde{q}}$ being the appropriate slepton and squark masses and p denoting particle four-momenta. In the case of the chargino exchange process $e^-u \to \tilde{\nu}\tilde{d}$ (fig. 1a), one substitutes the chargino masses m_{Ci} for m_i and the effective couplings $(\eta^C_{e_L,u_L})_i$ from eq. (23) for $(\eta_{e_a,q_b})_i$ in eq. (26) and uses the fact that $(\eta^C_{f_R})_i \equiv 0$. Similarly, in the case of the neutralino exchange processes $e^-q \to \tilde{e}^-\tilde{q}$ (fig. 1b) the appropriate substitutions are $m_i = m_{Ni}$ and $(\eta_{f_L,f_R})_i = (\eta^N_{f_L,f_R})_i$ where eq. (24) is to be used. Furthermore, the polarized differential cross sections for the processes

$$
\begin{aligned}
&e_a^-\bar{q}_b \to \tilde{\ell}_a\bar{\tilde{q}}_{b'}, \\
&e_a^+q_b \to \bar{\tilde{\ell}}_{a'}\tilde{q}_b, \\
&e_a^+\bar{q}_b \to \bar{\tilde{\ell}}_{a'}\bar{\tilde{q}}_{b'}
\end{aligned}
\tag{28}
$$

can be obtained from $d\sigma^{ab}(e^-q \to \tilde{\ell}\tilde{q})/d\hat{t}$ given in eqs. (25) and (26) by the following replacements:

$$
\begin{aligned}
&(\eta_{f_L})_i \to (\eta_{f_R})_i^* \qquad \text{if} \quad f_L \to \bar{f}_L, \\
&(\eta_{f_R})_i \to (\eta_{f_L})_i^* \qquad \text{if} \quad f_R \to \bar{f}_R.
\end{aligned}
\tag{29}
$$

For clarity, we note that in our notation $\bar{\tilde{f}}_R$ and $\bar{\tilde{f}}_L$ are the scalar partners of the left- and right-handed antifermions $\bar{f}_L$ and $\bar{f}_R$, respectively, so that the subscripts a and a′ (and, similarly, b and b′) specifying the processes (28) are just opposite to each other.

The integrated cross section for the production of a particular slepton-squark pair in unpolarized ep collisions at the c.m. energy $\sqrt{s}$ is obtained from the above polarized differential cross sections as follows:

$$
\sigma^{ab}(ep \to \tilde{\ell}\tilde{q}X) = \int_{x_{min}}^{1} dx \int_{\hat{t}_{max}}^{\hat{t}_{min}} d\hat{t}\, \tfrac{1}{4} \frac{d\sigma^{ab}(eq \to \tilde{\ell}\tilde{q})}{d\hat{t}} q(x, Q^2)
\tag{30}
$$

with the integration boundaries

$$
x_{min} = (m_{\tilde{\ell}} + m_{\tilde{q}})^2/s,
\tag{31}
$$

$$
\hat{t}_{\substack{min\\max}} = -\tfrac{1}{2}\left(sx - m_{\tilde{\ell}}^2 - m_{\tilde{q}}^2 \mp \sqrt{\left(sx - m_{\tilde{\ell}}^2 - m_{\tilde{q}}^2\right)^2 - 4m_{\tilde{\ell}}^2 m_{\tilde{q}}^2}\right).
\tag{32}
$$

The factor $\frac{1}{4}$ in eq. (30) arises from averaging over the incident lepton and quark polarizations. Furthermore, the function $q(x, Q^2)$ denotes the appropriate quark density (or antiquark density in the case of $e\bar{q} \to \tilde{\ell}\,\bar{\tilde{q}}$) of the proton, x being the fraction of the proton momentum carried by the (anti)quark and Q^2 being the QCD evolution scale for which we take

$$Q^2 = -\hat{t}. \tag{33}$$

Finally, the various production channels are indicated by $\mathrm{a, b} \in \{\mathrm{L, R}\}$ according to the notation used in eqs. (25), (26) and (28).

4. Numerical results

Having at hand suitable examples of chargino and neutralino spectra as well as the necessary analytical expressions of cross sections, we are now ready for numerical investigations. Thereby, we shall concentrate on the maximum ep center-of-mass energy provided by HERA [6], that is $\sqrt{s} = 314$ GeV, but for completeness we shall also make a brief excursion to higher energies. For the chargino and neutralino spectra we exclusively use solutions for $m_{\mathrm{N1}} \leqslant 100$ GeV derived with the constraints (15) as explained in sect. 2 and summarized in table 1. As far as the scalar masses are concerned, we shall study two cases. In the first case, slepton and squark masses are considered as basically free parameters in the sense that no theoretical mass relations are used. In the second case, we employ the renormalization group relations [5] for sparticle masses provided by the minimal supergravity model. Furthermore, for the quark densities we take set I of ref. [7] with the evolution scale (33). We have checked that the results do not change significantly, if the scale $Q^2 = -\frac{1}{2}(\hat{t}_{\mathrm{min}} + \hat{t}_{\mathrm{max}})$ with $\hat{t}_{\mathrm{min,\,max}}$ from eq. (32) is used as in refs. [3] and [4]. Finally, for the electroweak parameters we substitute the numerical values $\alpha = e^2/4\pi = \frac{1}{137}$, $\sin^2\theta_{\mathrm{W}} = 0.23$ and $m_{\mathrm{Z}} = m_{\mathrm{W}}/\cos\theta_{\mathrm{W}} = 93$ GeV.

4.1. PRODUCTION CROSS SECTIONS FOR UNCONSTRAINED SCALAR MASSES

Taking the attitude that slepton and squark masses are unknown parameters to be determined by experiment, we are free to make the choice

$$\begin{gathered} m_{\tilde{\nu}} = m_{\tilde{\mathrm{e}}_{\mathrm{L}}} = m_{\tilde{\mathrm{e}}_{\mathrm{R}}} = m_{\tilde{\ell}}, \\ m_{\tilde{\mathrm{u}}_{\mathrm{L}}} = m_{\tilde{\mathrm{u}}_{\mathrm{R}}} = m_{\tilde{\mathrm{d}}_{\mathrm{L}}} = m_{\tilde{\mathrm{d}}_{\mathrm{R}}} = m_{\tilde{\mathrm{q}}}, \end{gathered} \tag{34}$$

where $\tilde{\mathrm{u}}$ and $\tilde{\mathrm{d}}$ stand for all up- and down-type squark flavors, respectively. This simplification suffices for illustrative purposes. Furthermore, we define unpolarized total cross sections

$$\sigma(\mathrm{ep} \to \tilde{\ell}\tilde{\mathrm{q}}\mathrm{X}) = \sum_{\mathrm{a=L,R}} \sum_{\mathrm{b=L,R}} \sum_{\mathrm{q}} \sigma^{\mathrm{ab}}(\mathrm{ep} \to \tilde{\ell}\tilde{\mathrm{q}}\mathrm{X}) \tag{35}$$

by summing the cross sections for $\tilde{\ell}\tilde{\mathrm{q}}$ production given in eq. (30) with respect to the quark flavors present in the proton and the L- and R-sfermion species. Explicit calculation reveals that the cross sections depend, to a very good approximation, only on the sum $m_{\tilde{\ell}} + m_{\tilde{q}}$ of slepton and squark masses. This is expected from eq. (31) and the fact that the dominant contributions to the integral over x in eq. (30) come from the region $x \simeq x_{\min}$. Only if $m_{\tilde{\ell}} \ll m_{\tilde{q}}$ or $m_{\tilde{q}} \ll m_{\tilde{\ell}}$ deviations from this simple behaviour are observed. Therefore, one may conveniently take

$$m_{\tilde{\ell}} = m_{\tilde{q}} \tag{36}$$

in numerical calculations without loosing much of generality. More precisely, the cross sections for $m_{\tilde{\ell}} \neq m_{\tilde{q}}$ are the same as the ones for equal masses as long as $m_{\tilde{\ell}} + m_{\tilde{q}}$ takes the same value and $m_{\tilde{\ell}}$ and $m_{\tilde{q}}$ are not too different.

Fig. 2 shows predictions on the total cross sections (35) versus $m_{\tilde{\ell}} + m_{\tilde{q}}$ for HERA. Plotted are the results for four chargino/neutralino spectra selected from the solutions of table 1 with $m_{N1} \leqslant 100$ GeV including those which lead to maximum and minimum cross sections. Whereas for e^+p collisions the relative magnitude of the cross sections (a)–(d) follows the pattern one would naively expect from the masses of the wino-dominated chargino and the photino-dominated neutralino states of the spectra (a)–(d), the relative magnitude of the e^-p cross sections is less easy to explain due to a rather subtle interplay of valence and sea quark contributions. We note that the current lower limits on sparticle masses [8], to wit

$$\begin{aligned} &m_{\tilde{e}} \gtrsim \begin{cases} 20 \text{ GeV for } m_{\tilde{\gamma}} \simeq 20 \text{ GeV} \\ 60 \text{ GeV for } m_{\tilde{\gamma}} \simeq 0 \end{cases}, \\ &m_{\tilde{q}} \gtrsim 60 \text{ GeV}, \\ &m_{\tilde{W}} \gtrsim 20 \text{ GeV}, \end{aligned} \tag{37}$$

still allow cross sections at HERA as large as 10 pb. Here, the $\tilde{\gamma}$ and $\tilde{W}$ bounds should be applied to $\tilde{\chi}_{N1}$ and $\tilde{\chi}_{C1}$, respectively, except in the case (b) where $\tilde{\chi}_{N1}$ is essentially a higgsino and $\tilde{\gamma} \simeq \tilde{\chi}_{N2}$.

Another important question concerns the minimum production rates which are required for detection. The answer to this question depends first and foremost on the dominant decay modes of sleptons and squarks. Rather clear signatures are provided by the two-body decays $\tilde{e} \to e + \text{LSP}$ and $\tilde{q} \to q + \text{LSP}$ where LSP denotes the lightest supersymmetric particle which in the usual models is assumed to be stable. Since the LSP is invisible, the above decays give rise to large energy-momentum imbalances and thus allow a very efficient separation of SUSY events from the ordinary deep-inelastic scattering background due to $ep \to eqX$. This has been convincingly demonstrated in ref. [9] for the case $ep \to \tilde{e}\tilde{q}X$; $\tilde{e} \to e\tilde{\gamma}$, $\tilde{q} \to q\tilde{\gamma}$ where

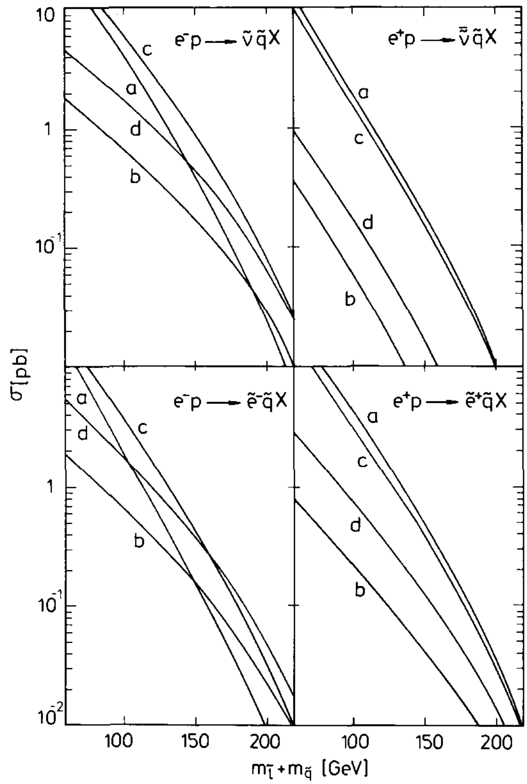

Fig. 2. Slepton-squark production cross sections at $\sqrt{s} = 314$ GeV versus $m_{\tilde{\ell}} + m_{\tilde{q}}$ for equal scalar masses and the mixing scenarios (masses in GeV) (a) $m_{N1} = 0$, $m_{C1} = 30$ ($M_2 = 0$, $\mu \simeq 192$); (b) $m_{N1} = 20$, $m_{C1} = 30$ ($M_2 \simeq 424$, $\mu \simeq 47$); (c) $m_{N1} = 20$, $m_{C1} = 50$ ($M_2 \simeq 36$, $\mu \simeq -410$); (d) $m_{N1} = 100$, $m_{C1} = 200$ ($M_2 \simeq 190$, $\mu \simeq -183$) specified further in table 1.

the LSP is identified with the (massless) photino. It was concluded that the standard NC background can be eliminated by suitable cuts without loosing more than about 20% of the signal. In that case, a rate of ten such events per year should be sufficient for detection. This implies a minimum cross section of 0.1 pb for the luminosity 10^{31} $\mathrm{cm}^{-2}\ \mathrm{s}^{-1}$ designed for HERA, provided $\tilde{e} \to e\tilde{\gamma}$ and $\tilde{q} \to q\tilde{\gamma}$ are the dominant decay modes. Although this situation is not unlikely, it is by no means guaranteed. Many other and more complicated decays may occur. For example, the LSP may be a higgsino or a sneutrino in which case one would expect $\tilde{e}$ and $\tilde{q}$ to decay through some cascades. Moreover, the gluino may be sufficiently light so that squarks decay dominantly through $\tilde{q} \to q\tilde{g}$ followed by $\tilde{g} \to q\bar{q} + \mathrm{LSP}$. Therefore, one should reckon with the possibility that a clear signal may only be obtained for cross sections somewhat larger than 0.1 pb. This particularly applies to the chargino exchange process $ep \to \tilde{\nu}\tilde{q}X$ with $\tilde{\nu} \to \nu + \mathrm{LSP}$ since both $\tilde{\nu}$ decay products are invisible. Some further discussion of such more complicated cases can be found in ref. [9].

From the above remarks it is clear that one cannot just straightforwardly deduce detection limits from the theoretical cross sections presented in fig. 2. One would rather need detailed Monte Carlo studies of the dominant decay processes for a given sparticle spectrum in order to draw definite conclusions. Nevertheless, it may be useful to at least indicate the reach of HERA by quoting the range of slepton and squark masses for which the larger one of the two cross sections $\sigma(e^{\mp}p \to \tilde{e}^{\mp}\tilde{q}X) \geqslant 0.1$ pb. The so-defined detection limits are

$$m_{\tilde{e}} + m_{\tilde{q}} \lesssim \begin{cases} 180\ \text{GeV} & \text{(a), (c), (d)} \\ 160\ \text{GeV} & \text{(b)} \end{cases}, \tag{38}$$

where (a)–(d) refer to the chargino and neutralino models considered in fig. 2. In fact, in the cases (a) and (c) the lightest neutralino $\tilde{\chi}_{N1}$ being a candidate for the LSP is essentially a photino. Hence, if $m_{\tilde{g}} > m_{\tilde{q}}$ one is in the favorable situation analyzed in ref. [9] which confirms the limit (38). On the other hand, in scenario (b) the lightest neutralino is approximately a higgsino while in scenario (d) the lightest neutralino $\tilde{\chi}_{N1} \simeq \tilde{\gamma}$ is so heavy that either $\tilde{e} \to e\tilde{\gamma}$ or $\tilde{q} \to q\tilde{\gamma}$ is forbidden for $m_{\tilde{e}} + m_{\tilde{q}} \lesssim 200$ GeV. Thus, in these two cases the limit (38) may be somewhat too optimistic.

4.2. PRODUCTION CROSS SECTIONS IN THE MINIMAL SUPERGRAVITY MODEL

In the framework of the minimal supergravity model, the $SU(3)_c \times SU(2)_L \times U(1)$ gaugino mass parameters M_3, M_2 and M_1 are related to a single mass parameter $m_{1/2}$ by renormalization group equations [2, 5] such as eq. (16). Assuming

$$M_3 = M_2 = M_1 = m_{1/2} \tag{39}$$

at the grand unification scale $M_X = 2.4 \times 10^{16}$ GeV and using $g_X^2/4\pi \simeq \frac{1}{24}$, $\alpha(m_W) \simeq \frac{1}{128}$ and $\alpha_s(m_W) \simeq 0.12$ one obtains

$$M_3 \simeq 2.9 m_{1/2} \quad \text{and} \quad M_2 \simeq 2M_1 \simeq 0.82 m_{1/2} \tag{40}$$

at energy scales of $O(m_W)$. M_2 and M_1 enter the chargino and neutralino mass matrices given in eqs. (7) and (8) and $M_3 = m_{\tilde{g}}$ is the effective gluino mass.

The model also provides renormalization group relations for scalar masses [5]. For equal Higgs vacuum expectation values $v_1 = v_2$ as assumed in (15a), these relations read

$$m_{\tilde{\nu}}^2 = m_{\tilde{e}_L}^2 \simeq m_0^2 + 0.23 M_1^2 + 0.73 M_2^2 ,$$

$$m_{\tilde{e}_R}^2 \simeq m_0^2 + 0.91 M_1^2 ,$$

$$m_{\tilde{u}_L}^2 = m_{\tilde{d}_L}^2 \simeq m_0^2 + 0.025 M_1^2 + 0.73 M_2^2 + 0.79 M_3^2 ,$$

$$m_{\tilde{u}_R}^2 \simeq m_0^2 + 0.4 M_1^2 + 0.79 M_3^2 ,$$

$$m_{\tilde{d}_R}^2 \simeq m_0^2 + 0.1 M_1^2 + 0.79 M_3^2 , \tag{41}$$

where the scalar mass parameter m_0 defined at M_X is the gravitino mass and M_1, M_2 and M_3 are as given in eq. (40). Contributions from Yukawa couplings to eq. (41) are neglected. These effects mainly shift the mass of the scalar top quark $\tilde{t}$ away from $m_{\tilde{u}}$ and induce small mixing between sfermions with the same charge. Combining eqs. (40) and (41) one arrives at the approximate slepton and squark mass relations [2]

$$m_{\tilde{\ell}_L}^2 \simeq m_0^2 + 0.5 m_{1/2}^2 , \qquad m_{\tilde{\ell}_R}^2 \simeq m_0^2 + 0.15 m_{1/2}^2 ,$$

$$m_{\tilde{q}_L}^2 \simeq m_{\tilde{q}_R}^2 \simeq m_0^2 + 7 m_{1/2}^2 . \tag{42}$$

To proceed, we choose values for the lightest neutralino and chargino masses m_{N1} and m_{C1}, diagonalize the mass matrices eqs. (7) and (8) under the assumptions (15) and determine the remaining neutralino and chargino masses, the eigenstates and the parameters M_2 and μ as explained in sect. 2. From M_2 and eq. (40) we get $m_{1/2}$ which is then substituted in eq. (42). Finally, using eq. (42) we compute the cross sections defined in eq. (35) as a function of m_0. Numerical results are depicted in fig. 3 for four choices (a)–(d) of m_{N1} and m_{C1} which are specified in the figure caption together with the corresponding values of $m_{1/2}$ and μ. From current SUSY searches one has deduced various limits [10] on the parameters $m_{1/2}$ and m_0 such as

$$m_0 \gtrsim 55 \text{ GeV} \qquad \text{for } m_{1/2} \simeq 20 \text{ GeV} \qquad (\text{a and b}),$$

$$m_0 \gtrsim 15 \text{ GeV} \qquad \text{for } m_{1/2} \simeq 40 \text{ GeV} \qquad (\text{c and d}). \tag{43}$$

These bounds are taken into account in fig. 3.

One sees that the maximum cross sections compatible with the existing constraints on the present model are of the order of 1 pb. On the other hand, as argued in subsect. 4.1 detection of slepton-squark production at HERA [9] should be possible for cross sections as small as about 0.1 pb. Thus, using the same criterion as

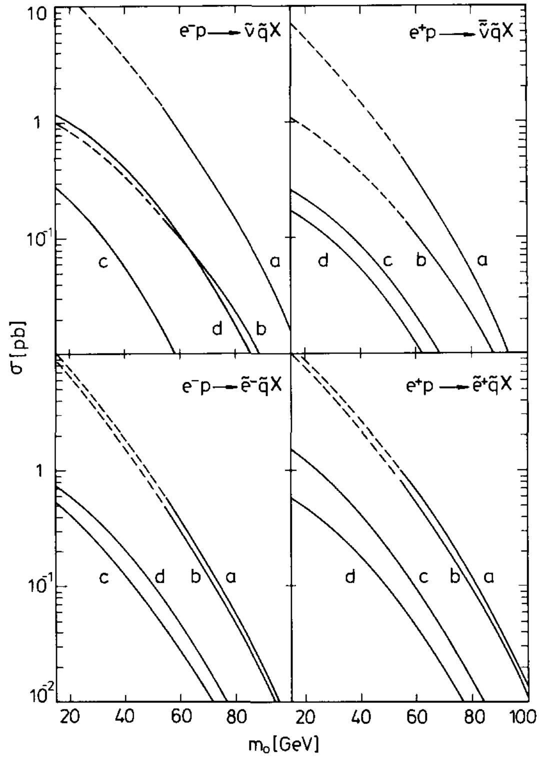

Fig. 3. Slepton-squark production cross sections at $\sqrt{s} = 314$ GeV versus the scalar mass parameter m_0 for the mixing scenarios (masses in GeV) (a) $m_{\mathrm{N1}} = 10$, $m_{\mathrm{C1}} = 30$ ($M_2 = 17.3$, $\mu = -493.2$); (b) $m_{\mathrm{N1}} = 10$, $m_{\mathrm{C1}} = 80$ ($M_2 = 16.4$, $\mu = -24.7$) (c) $m_{\mathrm{N1}} = 20$, $m_{\mathrm{C1}} = 30$($M_2 = 32.1$, $\mu = 77.3$); (d) $m_{\mathrm{N1}} = 20$, $m_{\mathrm{C1}} = 50$ ($M_2 = 35.5$, $\mu = -410.0$). The corresponding gaugino mass parameter $m_{1/2}$ is obtained from eq. (40) and takes the values (in GeV): (a) 21.0, (b) 20.0, (c) 39.1, (d) 43.3. The scalar masses $m_{\tilde{\ell}}$ and $m_{\tilde{q}}$ are related to m_0 and $m_{1/2}$ by the renormalization group equations (42). Cases incompatible with current experimental constraints are marked by dashed curves.

in eq. (38) in order to estimate detection limits from fig. 3 and eq. (42) one finds

$$m_{\tilde{\ell}} \lesssim 80\ \mathrm{GeV}, \qquad m_{\tilde{q}} \lesssim 100\ \mathrm{GeV} \qquad \text{for (a) and (b)},$$

$$m_{\tilde{\ell}} \lesssim 60\ \mathrm{GeV}, \qquad m_{\tilde{q}} \lesssim 120\ \mathrm{GeV} \qquad \text{for (c) and (d)}. \tag{44}$$

These values are consistent with the result (38) obtained for the previous model which is slightly more general. In addition, the gluino masses associated with the scalar masses (44) are fixed in the present model by eq. (40) yielding

$$m_{\tilde{g}} \simeq 60\ \mathrm{GeV} \qquad \text{for (a) and (b)},$$

$$m_{\tilde{g}} \simeq m_{\tilde{q}} \qquad \text{for (c) and (d)}. \tag{45}$$

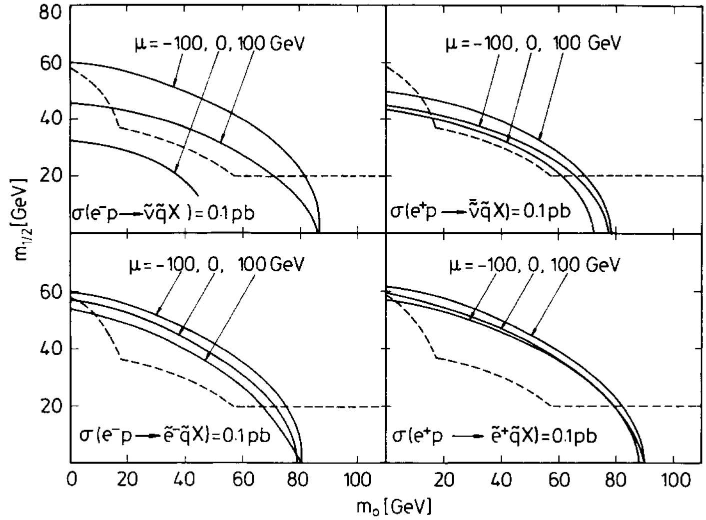

Fig. 4. Limits of SUSY searches at HERA ($\sqrt{s}$ = 314 GeV) in the framework of a minimal supergravity model. The full curves indicate the accessible range of the SUSY breaking parameters $m_{1/2}$, m_0 and μ if $\sigma(\mathrm{ep} \to \tilde{\ell}\tilde{\mathrm{q}}\mathrm{X}) \simeq 0.1$ pb is the smallest cross section for which a signal can be detected. The region in $(m_{1/2}, m_0)$ below the dashed curves is already excluded by present-day limits on sparticle masses.

Hence, in the cases (a) and (b) of fig. 3 squarks with masses $m_{\tilde{\mathrm{q}}} \simeq 100$ GeV decay via $\tilde{\mathrm{q}} \to \mathrm{q}\tilde{\mathrm{g}}$ and $\tilde{\mathrm{g}} \to \mathrm{q}\bar{\mathrm{q}} + \mathrm{LSP}$ producing a missing momentum signal which is less striking than the one from the direct decay $\tilde{\mathrm{q}} \to \mathrm{q} + \mathrm{LSP}$. As a consequence, we expect the detection limit for (a) and (b) to be somewhat lower than the one quoted in eq. (44).

The prospects of testing the minimal supergravity model at HERA are summarized in fig. 4. This figure shows the contours in the $(m_{1/2}, m_0)$-plane for which the cross sections defined by eq. (35) take the value $\sigma(\mathrm{eq} \to \tilde{\ell}\tilde{\mathrm{q}}\mathrm{X}) = 0.1$ pb. Here, the higgsino mass parameter μ is restricted to the range $|\mu| \leqslant 100$ GeV. However, as expected and quantified in fig. 4, the value of μ does not have a decisive influence on the size of the cross section. For comparison, we also indicate the current limits [10] on $m_{1/2}$ and m_0 derived from the non-observation of the processes $\mathrm{e}^+\mathrm{e}^- \to \tilde{\mathrm{e}}^+\tilde{\mathrm{e}}^-$, $\mathrm{e}^+\mathrm{e}^- \to \tilde{\gamma}\tilde{\gamma}\gamma$ and of $\tilde{\mathrm{g}}$ production at the CERN collider. It becomes quite evident from our analysis that the minimal supergravity model can be tested at HERA only in a relatively small region of the parameter space beyond the present bounds.

4.3. UNPOLARIZED ASYMMETRIES

If a sufficiently strong signal of slepton-squark production is found, there are several ways to extract information on the exchanged chargino and neutralino

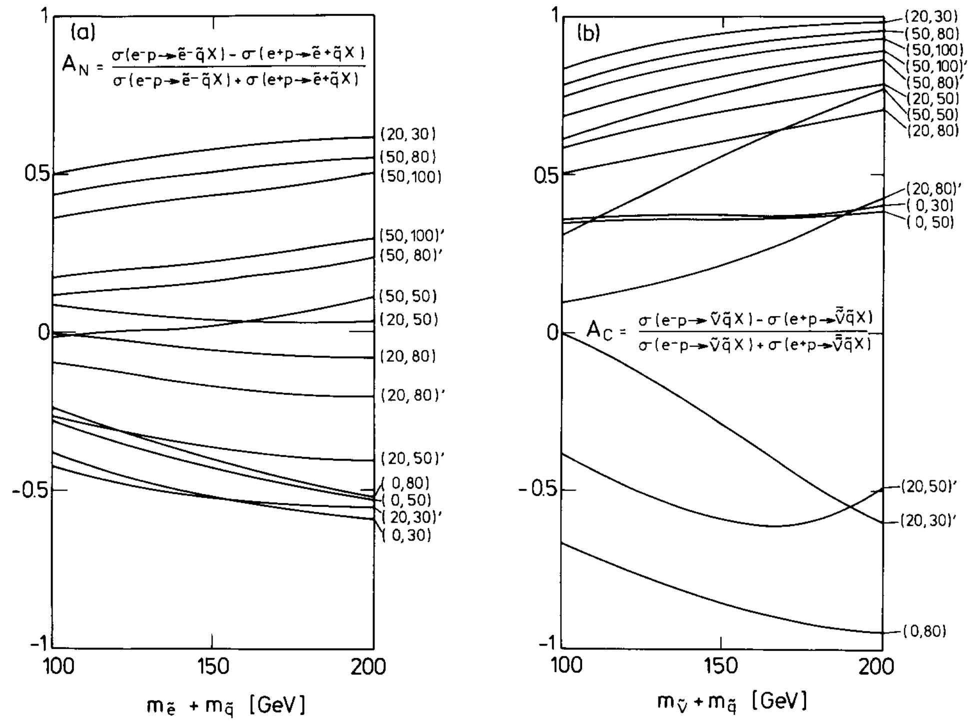

Fig. 5. Asymmetries of (a) $\tilde{e}\tilde{q}$ and (b) $\tilde{\nu}\tilde{q}$ production in $e^{\mp}p$ collisions at $\sqrt{s} = 314$ GeV versus $m_{\tilde{\ell}} + m_{\tilde{q}}$ for equal scalar masses and all mixing scenarios of table 1 with $m_{N1} \leqslant 150$ GeV. The numbers in the brackets give the values of m_{N1} and m_{C1} in GeV with $(\cdots)$ and $(\cdots)'$ referring to the first and second solution, respectively.

states. As obvious from figs. 2 and 3 some insight could be gained directly from the size of the production cross sections. However, since the latter are steep functions of the slepton and squark masses, such an attempt would require a sufficiently precise mass determination in addition to the knowledge of the branching ratios of the observed decay modes.

Another possibility, which does not need beam polarization, is investigated in fig. 5. These plots show the asymmetries

$$A_N = \frac{\sigma(e^-p \to \tilde{e}^-\tilde{q}X) - \sigma(e^+p \to \tilde{e}^+\tilde{q}X)}{\sigma(e^-p \to \tilde{e}^-\tilde{q}X) + \sigma(e^+p \to \tilde{e}^+\tilde{q}X)}, \tag{46}$$

$$A_C = \frac{\sigma(e^-p \to \tilde{\nu}\tilde{q}X) - \sigma(e^+p \to \bar{\tilde{\nu}}\tilde{q}X)}{\sigma(e^-p \to \tilde{\nu}\tilde{q}X) + \sigma(e^+p \to \bar{\tilde{\nu}}\tilde{q}X)} \tag{47}$$

in the total slepton-squark production in e^-p versus e^+p collisions as specified in eq. (35). From this demonstration in which all neutralino and chargino spectra of table 1 with $m_{N1} \leqslant 50$ GeV are considered we learn that the above charge asymmetries are very sensitive to neutralino and chargino properties, while they depend only relatively weakly on the slepton and squark masses in the interesting range $m_{\tilde{\ell}} + m_{\tilde{q}} \gtrsim 100$ GeV. Both facts make these observables particularly useful for testing the neutralino and chargino sector at HERA in case a $\tilde{\ell}\tilde{q}$ signal is observed. Moreover, tests based on ratios such as eqs. (46) and (47) profit by cancellations of uncertainties in the experimental cross section determinations arising from systematic errors and a priori unknown $\tilde{\ell}$ and $\tilde{q}$ branching fractions. It is clear from fig. 5 that even a rough measurement of A_N and A_C would sort out a particular class of neutralino and chargino solutions and thus provide valuable information on gaugino-higgsino mixing, that is on SUSY and electroweak symmetry breaking.

Finally, we want to mention the existence of various asymmetries in $\tilde{\ell}\tilde{q}$ production with longitudinally polarized $e^{\pm}$ beams [4,11]. Measurements of polarization asymmetries, which may indeed become possible at HERA [6], would shed light on further details of the neutralino/chargino sector and on the mass difference between $\tilde{e}_L$ and $\tilde{e}_R$.

4.4. SLEPTON-SQUARK PRODUCTION AT HIGHER ENERGIES

We conclude our numerical studies with a brief outlook for slepton and squark production at energies beyond the HERA c.m. energy range [12]. Fig. 6 exemplifies the rise of the production cross sections with the ep collision energy. The parameters of these examples are chosen in accordance with the specifications of subsect. 4.1, but in such a way that they are also roughly consistent with the mass relations (40) and (42) of the minimal supergravity model considered in subsect. 4.2. The appropriate values of $m_{1/2}$ and m_0 to be substituted in these relations are

$$\begin{aligned} &\text{(a)} && m_{1/2} \simeq 40 \text{ GeV}, && m_0 \simeq 40 \text{ GeV}, \\ &\text{(b)} && m_{1/2} \simeq 100 \text{ GeV}, && m_0 \simeq 70 \text{ GeV}, \\ &\text{(c)} && m_{1/2} \simeq 230 \text{ GeV}, && m_0 \simeq 100 \text{ GeV}. \end{aligned} \tag{48}$$

For definiteness, we shall concentrate on the c.m. energy $\sqrt{s} \simeq 1.3$ TeV which would be provided by collisions of 50 GeV electrons from LEP with 8.5 TeV protons from LHC, the pp collider project in the LEP tunnel. For this ep option we assume the luminosity $L = 10^{32}\ \text{cm}^{-2}\ \text{s}^{-1}$ as suggested by detailed machine studies [13]. It is then reasonable to take 10^{-2} pb as the smallest cross section for which a signal can be detected. In that case, one would be able to reach sparticle masses up to

$$m_{\tilde{\ell}} + m_{\tilde{q}} \simeq 700 \text{ GeV} \tag{49}$$

as indicted by fig. 6.

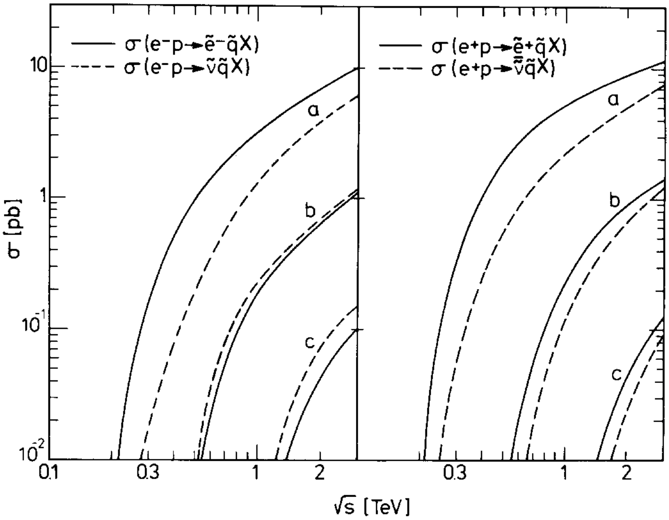

Fig. 6. Slepton-squark production cross sections versus the ep c.m. energy $\sqrt{s}$ for the following mixing scenarios (see table 1) and scalar masses (in GeV): (a) $m_{\mathrm{N1}} = 20$, $m_{\mathrm{C1}} = 50$ ($M_2 \simeq 33$, $\mu \simeq 31$), $m_{\tilde{\ell}} = 50$, $m_{\tilde{q}} = 100$; (b) $m_{\mathrm{N1}} = 50$, $m_{\mathrm{C1}} = 100$ ($M_2 \simeq 87$, $\mu \simeq -64$), $m_{\tilde{\ell}} = 100$, $m_{\tilde{q}} = 250$; (c) $m_{\mathrm{N1}} = 100$, $m_{\mathrm{C1}} = 200$ ($M_2 \simeq 190$, $\mu \simeq -183$), $m_{\tilde{\ell}} = 150$, $m_{\tilde{q}} = 600$.

5. Concluding remarks

In ep collisions, the occurrence of processes such as $\mathrm{eq} \to \tilde{\ell}\tilde{\mathrm{q}}$, $\mathrm{e}\gamma \to \tilde{\ell}\tilde{\chi}$, $\gamma\mathrm{q} \to \tilde{\mathrm{g}}\tilde{\mathrm{q}}$ and $\gamma\mathrm{g} \to \tilde{\mathrm{q}}\bar{\tilde{\mathrm{q}}}$ would be a clear manifestation of supersymmetry. Additional, but less direct evidence would be provided by effects of squarks and gluinos on the running of the strong coupling constant $\alpha_s(Q^2)$, and by changes to the deep-inelastic structure functions due to the evolution of a $\tilde{\mathrm{q}}$ and $\tilde{\mathrm{g}}$ sea inside the proton. However, in view of the current limits on sparticle masses some of these possibilities appear to be beyond or already quite close to the limit of observability [14]. It is the associated production of sleptons and squarks which will probably play the most important role in SUSY searches at future ep colliders.

In agreement with other studies we find that at the c.m. energy $\sqrt{s} = 314$ GeV and with the luminosity $L = 10^{31}\ \mathrm{cm}^{-2}\ \mathrm{s}^{-1}$ provided by HERA one may be able to reach slepton and squark masses up to $m_{\tilde{\ell}} + m_{\tilde{q}} \simeq 180$ GeV. Our estimates further indicate that ep collisions at $\sqrt{s} = 1.3$ TeV should give access to scalar masses in the range $m_{\tilde{\ell}} + m_{\tilde{q}} \simeq 700$ GeV provided the luminosity is increased to $L = 10^{32}\ \mathrm{cm}^{-2}\ \mathrm{s}^{-1}$. In order to give more precise discovery limits one must pay attention to the considerable model-dependence of the cross sections for $\mathrm{ep} \to \tilde{\ell}\tilde{\mathrm{q}}\mathrm{X}$ and carefully investigate the decay signatures of $\tilde{\ell}$ and $\tilde{\mathrm{q}}$. On the theory side, the main uncertainties arise from the unknown masses and mixing angles of the neutralino and chargino states and from the gluino mass. We have clarified the problem concerning the production cross sections in the minimal supersymmetric extension of the standard model with and without supergravity mass relations. The numerical examples shown give a fairly detailed account of slepton-squark production for the experimentally relevant range of parameters.

Finally, it is interesting to compare the discovery potential of HERA with the prospects for detecting selectrons at LEP and squarks at the Tevatron, although such a comparison should be made with caution. Similarly as present-day e^+e^- machines, LEP will allow to test the existence of selectrons with masses almost as large as the beam energy that is $m_{\tilde{e}} \simeq 40$ GeV at LEP I [15] and $m_{\tilde{e}} \simeq 90$ GeV at LEP II [16]. Stronger limits are possible, but more model-dependent. Squarks, on the other hand, are expected [17] to be detectable at the Tevatron $\bar{p}p$ collider up to masses $m_{\tilde{q}} \simeq 120$–200 GeV. There will thus be a considerable overlap of SUSY searches at these machines and at HERA which is useful to establish a clear signal or to put new stringent bounds on sparticle masses. Not to forget, these searches are also complementary in the sense that they test different fundamental couplings among ordinary and supersymmetric particles.

Note added

An initial brief account of our work was given in ref. [14]. While this paper was written up, we received a preprint by Bartl et al. [18], in which the production and decay of selectrons and squarks in ep collisions is studied and numerical results are given for three cases of gaugino-higgsino mixing with $v_1 = 0.9v_2$.

References

[1] H.P. Nilles, Phys. Reports 110 (1984) 1;
H.E. Haber and G.L. Kane, Phys. Reports 117 (1985) 75
[2] J. Ellis, Proc. Int. Symp. on Lepton and Photon Interactions at High Energies, Kyoto, 1985, eds. M. Konuma and K. Takahashi (Kyoto University, Kyoto, 1986) p. 850;
E. Reya, Proc. XXIII Int. Conf. on High Energy Physics, Berkeley, 1986, ed. S.C. Loken (World Scientific, Singapore, 1987) p. 285
[3] S.K. Jones and C.H. Llewellyn Smith, Nucl. Phys. B217 (1983) 145
[4] P.R. Harrison, Nucl. Phys. B249 (1985) 704
[5] K. Inoue, A. Kakuto, H. Komatsu and S. Takeshita, Prog. Theor. Phys. 68 (1982) 927; 71 (1984) 413;
J. Ellis, J.S. Hagelin, D.V. Nanopoulos and K. Tamvakis, Phys. Lett. 125B (1983) 275;
L. Alvarez-Gaumé, I. Polchinski and M.B. Wise, Nucl. Phys. B221 (1983) 495;
L.E. Ibáñez and C. López, Phys. Lett. 126B (1983) 54; Nucl. Phys. B233 (1984) 511;
C. Kounnas, A.B. Lahanas, D.V. Nanopoulos and M. Quirós, Phys. Lett. 132B (1983) 95; Nucl. Phys. B236 (1984) 438
[6] Reports at the 13. Int. Accelerator Conf., Novosibirsk, 1986, DESY M-86-10
[7] E. Eichten, I. Hinchliffe, K. Lane and C. Quigg, Rev. Mod. Phys. 56 (1984) 579; and (E) 85 (1986) 1065
[8] M. Davier, Proc. XXIII Int. Conf. on High Energy Physics, Berkeley, 1986, ed. S.C. Loken (World Scientific, Singapore, 1987) p. 25

[9] R.J. Cashmore et al., Phys. Reports 122 (1985) 275
[10] J. Ellis and F. Pauss, Proc. Workshop on Physics at Future Accelerators, La Thuile and CERN, 1987, ed. J.H. Mulvey, CERN 87-07, vol. I, p. 80
[11] J. Bartels and W. Hollik, Communication to the Working Group on Exotic Physics at HERA, DESY, 1987
[12] G. Altarelli, B. Mele and R. Rückl, Proc. ECFA-CERN Workshop on Large Hadron Collider in the LEP Tunnel, Lausanne and CERN, 1984, ed. M. Jacob, CERN 84-10, vol. II, p. 551;
J.A. Bagger and M.E. Peskin, Phys. Rev. D31 (1985) 2211 and (E) D32 (1985) 1260
[13] G. Brianti, Proc. Workshop on Physics at Future Accelerators, La Thuile and CERN, 1987, ed. J.H. Mulvey, CERN 87-07, vol. I, p. 6
[14] R. Rückl, Physics at HERA, presented at the ECFA-Workshop LEP 200, Aachen, 1986, DESY 87-021;
R. Rückl, Proc. 13. Int. Winter Meeting on Fundamental Physics, Cuenca, 1985, eds. M. Aguilar-Benitez and A. Ferrando, (Instituto de Estudios Nucleares, Madrid, 1986) p. 288
[15] H. Baer et al., Physics at LEP, eds. J. Ellis and R.D. Peccei, CERN 86-02, vol. 1, p. 297
[16] C. Dionisi, Supersymmetric particles search at LEP 200, presented at the ECFA-Workshop LEP 200, Aachen, 1986
[17] H. Baer and E.L. Berger, Phys. Rev. D34 (1986) 1361;
E. Reya and D.P. Roy, Z. Phys. C32 (1987) 615
[18] A. Bartl, H. Fraas and W. Majerotto, HEPHY-PUB 503/87